Computational and Theoretical Chemistry 1199 (2021) 113194

Contents lists available at ScienceDirect

Computational and Theoretical Chemistry

journal homepage: www.elsevier.com/locate/comptc

Structural phase diagram and bonding patterns of B_xH_y ($x + y = 20$) binary systems: A theoretical investigation

Chang Xu [a,b,*], Longjiu Cheng [a]

[a] Department of Chemistry, Key Laboratory of Functional Inorganic Materials of Anhui Province, Anhui University, Hefei, Anhui 230601, People's Republic of China
[b] Hefei National Laboratory for Physics Sciences at the Microscale, University of Science and Technology of China, Hefei, Anhui 230026, People's Republic of China

ARTICLE INFO

Keywords:
Borane cluster
Energy landscape
Localized chemical bonding
Multi-center bond

ABSTRACT

The borane clusters exhibit diverse geometries related with their special multi-center bonding patterns in different B/H ratios, due to the electronic deficiency character of boron atom. In this paper, global minimal structures of B_xH_y ($x + y = 20$) are predicted using unbiased structural search programs and their structural phase diagram is plotted. Relative energies of these clusters go down firstly and then rise up with $B_{10}H_{10}$ as the turning point, and $B_{12}H_8$, $B_{16}H_4$, B_{20} are magic numbers. The geometries of these clusters undergo the transition of 3D open cage – 3D closed cage – irregular 3D – 2D planar/quasi-planar along with the increasing B/H ratios, and their stability depends on flexibility of the multi-center bonding patterns. This study reveals the geometric evolution rule related with the electronic shells of B—H binary systems, which makes sense in borane chemistry.

1. Introduction

Boron element, which is next to carbon in the periodic table, has the electronic deficiency character, which leads to the formation of special multi-center chemical bonding patterns in boron-based clusters. In 1950s, the theory of hydrogen-bridge bonding pattern was proposed by Lipscomb and coworkers [1,2], in which they pointed out that three-center two-electron (3c-2e) B—H—B hydrogen bridge bond plays an important part in electronic stability of borane clusters. This theory revealed the nature of electronic shells in boranes, and after that plenty of borane clusters were reported experimentally and theoretically, the number of which is only next to hydrocarbon clusters.

The neutral all boron clusters B_n [3–6] and the cationic B_n^+ clusters [7] undergo the 2D-3D structural transition at $n = 20$ and $n = 16$ respectively, except for the flat cage B_{14} [8], whereas their anions keep the planar or quasi-planar structure until $n = 28$ [9–15]. However, the presence of hydrogen atoms would change geometries of these clusters. Recent studies revealed that B_nH_m clusters were planar/quasi-planar when $m < n$ [16–19]. Li and coworkers [20,21] theoretically investigated a series of borane clusters, and the results indicated that the B_nH_2 ($n = 4, 6, 8, 10, 12$) and $B_nH_2^-$ ($n = 3, 5, 7, 9, 11$) were planar double rings [22], and $B_{3n}H_m$ clusters, such as $B_{30}H_8$ and $B_{39}H_9^{2-}$, also had planar configuration, which were confirmed by photoelectron spectroscopy (PES) researches [23]. Chemical bonding analysis revealed that these borane clusters had similar delocalized multi-center bonding patterns and aromaticity as hydrocarbon clusters [24–26]. Interestingly, Li et al. [27] also pointed out that some planar borane clusters with twin-hexagonal holes, such as $B_{26}H_8$, could be the building blocks of stable boron sheets. Further hydrogenation of planar borane cluster would break its peripheral B-B σ bonds, causing the structural transition [28]. Böyükata and coworkers [29] revealed the effect of the hydrogens hosting on the B_5-B_{10} cages in B_nH_m ($m = 5$–10, $n \leq m$), of which the structures underwent the 2D-3D transition when $n = m$ [30]. Moreover, the structures of borane anions $B_nH_n^{2-}$ were also proved to be 3D [31,32], such as icosahedral $B_{12}H_{12}^{2-}$ [33,34]. They are classic borane series obtained in the early experiments, and their multi-center bonding patterns were discussed by Cheng *et al.* [35]. Toshihiko group [36] pointed out that dehydrogenation of $B_{12}H_n^+$ clusters would cause their 3D-2D structural transition, and their 3D structures keep the lower energy level when $n \geq 6$. Other investigations revealed that $B_{12}H_n^{0/-}$ underwent the 2D-3D structural transition when $n = 4$–5 [37], and this transition occurred for $B_6H_y^-$ when $y = 4$ [38].

Electronic shells of boranes were widely discussed to give the major consideration of the nature of their stability [39,40]. Localized molecule orbitals (LMOs) analysis was first proposed by Lipscomb and co-workers [41–44] to investigate the bonding patterns in small boranes. Recently,

* Address: Department of Chemistry, Key Laboratory of Functional Inorganic Materials of Anhui Province, Anhui University, Hefei, Anhui 230601, People's Republic of China.
E-mail addresses: xuchang1986@ahu.edu.cn (C. Xu), clj@ustc.edu (L. Cheng).

https://doi.org/10.1016/j.comptc.2021.113194
Received 25 November 2020; Received in revised form 18 February 2021; Accepted 18 February 2021
Available online 4 March 2021

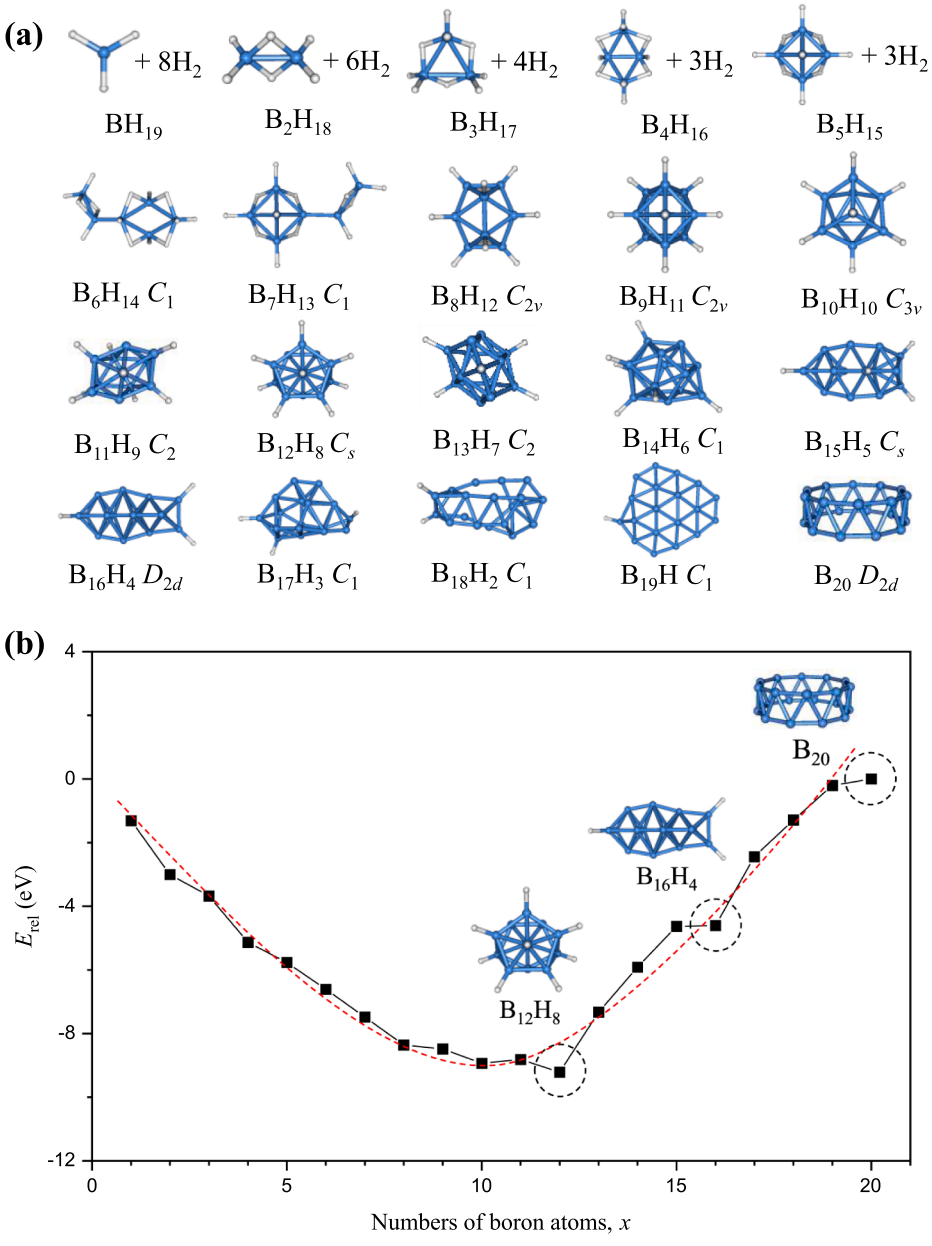

Fig. 1. (a) Global minimal structures of B_xH_y ($x + y = 20$) systems optimized at TPSSh/6-311+G** level of theory, when $x \leq 5$, the separate hydrogen molecules in the systems are not shown (B in blue and H in white, the symmetries are labeled below each structure) (b) Structural phase diagram (SPD) of B_xH_y ($x + y = 20$) systems, E_{rel} is their energies relative to B_{20} and H_2 at TPSSh/6-311+G** level, and the structures for three magic numbers are labeled (The variation trend is represented by the red dash line, $B_{12}H_8$, $B_{16}H_4$ and B_{20} are marked as the magic numbers).

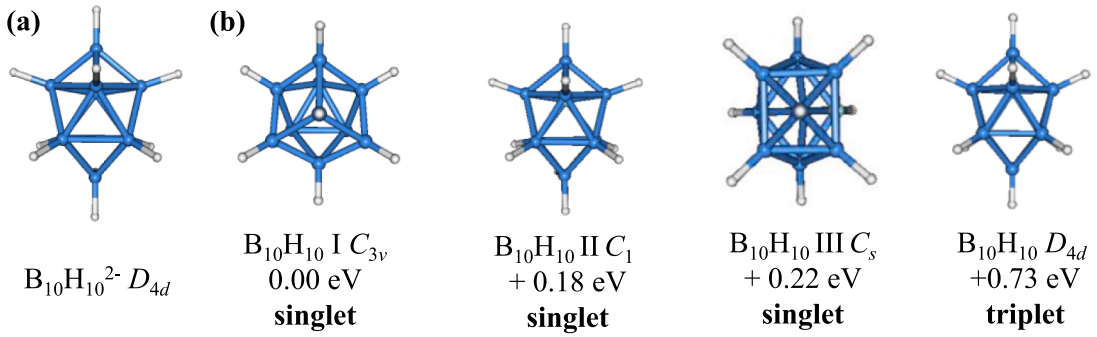

Fig. 2. (a) Global minimum structures of $B_{10}H_{10}^{2-}$ and (b) three low-lying isomers of $B_{10}H_{10}$ in singlet states and D_{4d} $B_{10}H_{10}$ in triplet state optimized from its dianion at TPSSh/6-311+G** level of theory (B in blue and H in white, symmetries and relative energies are labeled below each structure).

the AdNDP program [45] was developed by Boldyrev group to give further insight into LMOs in nanostructures. They investigated the bonding patterns of B_nH_{n+2} and pointed out that the boron atoms avoided sp^2 hybridization but formed the multi-center chemical bonds in these clusters [46]. The topological patterns of borane were also investigated by researchers to reveal their geometric characters, which indicated that these clusters could be classified into 4 types by Wade's rule – *closo-*, *nido-*, *arachno-* and *hypho-*, due to the relationships between the numbers of their skeleton boron atoms and valence electrons [47–50]. As there are multi-center delocalized systems in polyhedral borane, their 3D aromaticity was discussed by researchers [51–57].

Although plenty of experimental and theoretical reports of boranes have been proposed in recent years, there are little studies focusing on their potential energy surface. Energies and geometric characters are critical for the properties of clusters, and their comprehensive evolution rules could be revealed by the structural phase diagram (SPD). In this paper, we intent to investigate borane clusters with different B/H ratios through SPD. As the double ring B_{20} is the 2D-3D turning point of neutral boron clusters with special high stability [3,58,59], B_xH_y ($x + y = 20$) systems are chosen as the objects of our study. Their potential energy surface is searched theoretically, and the SPD is plotted to give insight into their stabilities and geometric evolution rules. In order to reveal the mechanism of their structural transition, the multi-center bonding patterns in their electronic shells are discussed.

2. Computational details

The global minimal structures of B_xH_y ($x + y = 20$) are searched by genetic algorithm (GA) coupled with density functional theory (DFT) method at TPSSh [60]/3-21G level, and further optimized using 6-311+G** basis set. The global search programs used in this study is developed by our group [61], in which the results of DFT calculation are called by main program of GA to carry out the global search (details could be found in Ref. [61]). The energies of these clusters are also calculated at the same level of theory. These methods have been proved to be reliable for main group elements [62–64]. Moreover, the bonding patterns of B_xH_y ($x + y = 20$) are investigated using the adaptive natural density partitioning (AdNDP) programs [45,65,66]. All calculations are carried out using the Gaussian 09 package [67], and molecular orbitals (MO) visualization is performed by Molekel 5.4 [68].

3. Results and discussions

3.1. Structural optimization

The low-lying isomers of B_xH_y ($x + y = 20$) are searched by GA/DFT method and further optimized (see Figs. S1–S4 of Supporting Information (SI)), and their global minimal structures are shown in Fig. 1(a) (Cartesian coordinates are given in Table S1 of SI)). The clusters in both singlet and triplet states are considered in our global search programs, and all the global minimums are proved to be singlet. As the number of hydrogen atoms is excessive in the optimized systems when $x \leq 5$, these systems are composed of separate hydrogen molecules and small classic borane clusters. BH_{19} system contains eight hydrogen molecules and the BH_3 cluster which is the smallest borane molecule. B_2H_{18} system is comprised of six hydrogen molecules and the D_{2h} B_2H_6 cluster. B_3H_{17} system contains four hydrogen molecules and the C_{3v} *arachno*-B_3H_9. B_4H_{16} system contains three hydrogen molecules and the C_{2v} *arachno*-B_4H_{10}. B_5H_{15} system is composed of three hydrogen molecules and the C_{4v} *nido*-B_5H_9. All these global minimums of B_xH_y ($x + y = 20$, $x \leq 5$) are plotted in Fig. 1(a), in which the separate hydrogen molecules are not shown.

Some of these small classic borane clusters – BH_3, B_2H_6, B_4H_{10}, B_5H_9, and B_5H_{11} have already been obtained in the experimental studies [1,2,69–71], which confirmed the reliability of our theoretical method. As we know, $B_{10}H_{10}^{2-}$ is a classic *closo*-borane cluster with D_{4d} symmetry (as shown in Fig. 2(a)) which follows the Wade's Law [47]. However, in our global search, the C_{3v} structure in singlet state (the first structure in Fig. 2(b)) is the global minimum for neutral $B_{10}H_{10}$, and its electronic shell is totally different form the D_{4d} $B_{10}H_{10}^{2-}$. When an electron-pair is lost in D_{4d} $B_{10}H_{10}^{2-}$, the neutral $B_{10}H_{10}$ in singlet state is obtained (the second structure in Fig. 2(b)), it has the C_1 symmetry with a little distortion from D_{4d} structure, due to Jahn-Teller effect. Its energy is 0.18 eV higher than the global minimum. Moreover, when two single electrons are lost in the $B_{10}H_{10}^{2-}$, the neutral $B_{10}H_{10}$ with open shell orbitals is obtained (the fourth structure in Fig. 2(b)), which is in triplet state. After optimization, its structure keeps D_{4d} symmetry, and its energy is 0.73 eV higher than the global minimum, and also higher than all the first three local minimal structures in singlet states (the first three structures in Fig. 2(b)).

3.2. Structural phase diagram

In order to reveal the rule of geometric evolution related with energies for B—H binary systems, the structural phase diagram of B_xH_y ($x + y = 20$) is plotted in Fig. 1(b), in which the E_{rel} is defined as:

$$E_{rel} = E_{B_xH_y} - \frac{xE_{B_{20}}}{20} - \frac{yE_{H_2}}{2} \quad (1)$$

$E(B_xH_y)$, $E(B_{20})$ and $E(H_2)$ are the energies of B_xH_y、B_{20} and H_2, respectively. Thus, the E_{rel} represents the energy of B_xH_y relative to B_{20} and H_2 and its value indicates the relative stability of these clusters, in which the more negative E_{rel} value means the higher stability.

The shape of SPD indicates that, as the B/H ratio increases, the relative energies of these systems (Table S2) go down firstly and then rise up with $B_{10}H_{10}$ as the turning point, and the E_{rel} values exhibit the

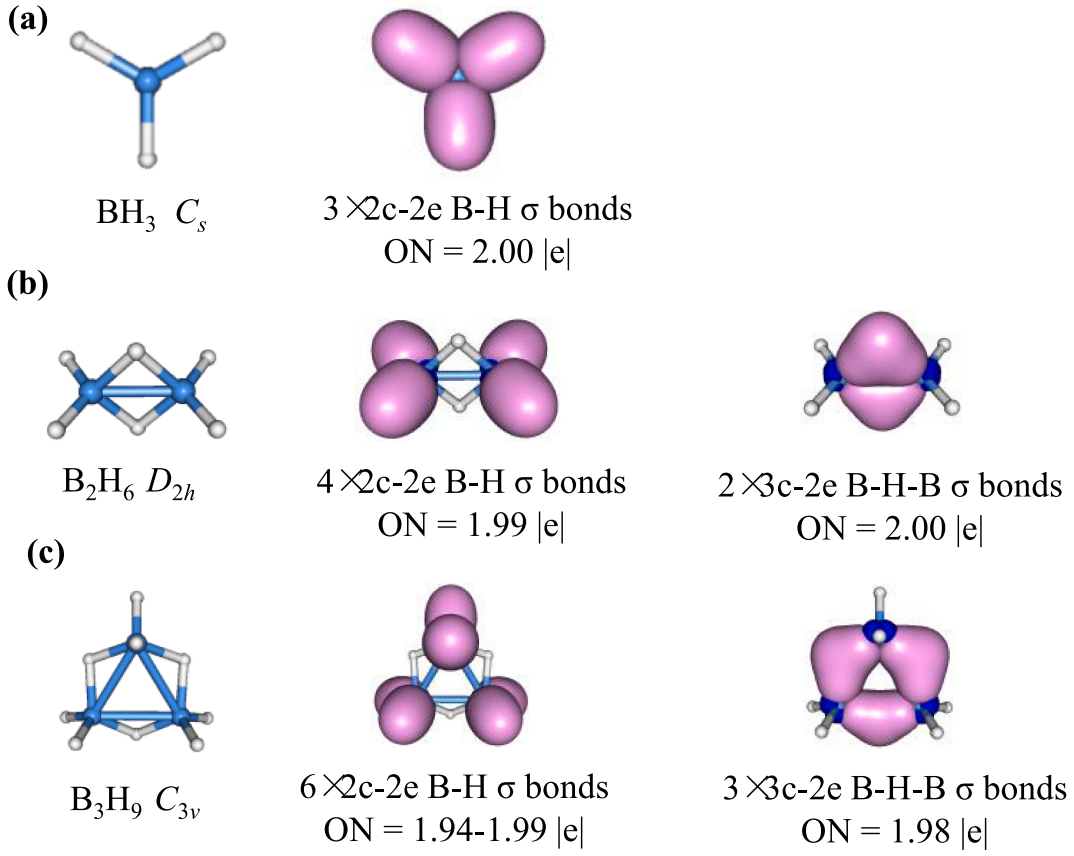

Fig. 3. Optimized structures and AdNDP chemical bonding of (a) BH_3 (b) B_2H_6 and (c) B_3H_9 (B in blue and H in white, symmetries and occupy numbers are labeled below each structure).

significant fluctuations when $x = 12$, $x = 16$ and $x = 20$, which exhibit extra high stability. When $x = 12$, there is a distorted icosahedral B_{12} core in the $B_{12}H_8$ structure, of which the E_{rel} decreases visibly. When $x = 16$, the $B_{16}H_4$ cluster could be viewed as the D_{2d} B_{14} [8] in which two terminal boron atoms are replaced by the HB-BH groups respectively (Fig. S5). As the B_{14} cage is the magic number of neutral boron clusters, the $B_{16}H_4$ keeps higher stability. The classic double ring B_{20} cluster is the 2D-3D turning point for neutral boron clusters [3,58,59]. Theoretical investigations reveal that there are two directional delocalized chemical bonds in its electronic structure, causing the double aromaticity and high stability. Therefore, $B_{12}B_8$, $B_{16}H_4$ and B_{20} are magic numbers in the B_xH_y ($x + y = 20$) series.

The rule of their geometric evolution is also revealed in the SPD result. The B_xH_y ($x + y = 20$) exhibit the 3D open cage structure when $3 \leq x \leq 9$. As the B/H ratio increases, their geometries turn to 3D closed cage when $10 \leq x \leq 16$. Then the clusters trend to keep irregular 3D structures when $x = 17$ and $x = 18$. Finally, they are transformed into planar/quasi-planar structures when $x = 19$ and $x = 20$, in which the double ring B_{20} could be viewed as the folded 2D ribbon. Moreover, all the low-lying isomers in Figs. S1–S4 keep the 3D open/closed cage structures when $x \leq 16$, and the stable planar/quasi-planar structures appear in the low-lying isomers when $x = 17$ and $x = 18$. When $x = 19$, global minimum of $B_{19}H$ has the quasi-planar structure, indicating the occurrence of their structural transition.

3.3. Chemical bonding analysis

In order to give insight into the nature of the structural transition for B_xH_y ($x + y = 20$), their chemical bonding patterns are further discussed. As the electronic deficiency character of boron atom, special multi-center bonding pattern exist in boranes. In 2008, the AdNDP programs depending on the natural bond orbital (NBO) theory was developed by Boldyrev and co-workers [45,65,66] for investigations of multi-center bonds, which is used to discuss the localized bonding patterns of B_xH_y ($x + y = 20$) clusters in our study.

3.3.1. B_xH_y ($x + y = 20$, $x \leq 5$)

When $x \leq 5$, the B_xH_y ($x + y = 20$) systems are composed of the classic borane clusters and separate hydrogen molecules. As mentioned above, BH_3, B_2H_6, B_3H_9, B_4H_{10} and B_5H_9 are global minimums, their AdNDP chemical bonding are shown in Fig. 3(a)–(c) and Fig. 4(a) and (b). As the smallest borane molecule, BH_3 contains three B—H σ bonds (Fig. 3(a)). B_2H_6 (D_{2h}) and *arachno*-B_3H_9 (C_{3v}) are formed by B—H single bonds and B—H—B hydrogen-bridge bonds (Fig. 3(b) and (c)). As the ratio of B/H increases, multi-center B_n bonds appear in the *arachno*-B_4H_{10} (C_{2v}) and *nido*-B_5H_9 (C_{4v}). Beside B—H and B—H—B bonds, there are one 4c-2e σ B_4 bond in B_4H_{10} (Fig. 4(a), details of 4c-2e B_4 bond are shown in Fig. S6), and two 5c-2e π and one 5c-2e σ B_5 bonds in B_5H_9 (Fig. 4(b)). From the geometry structures, the clusters could be viewed

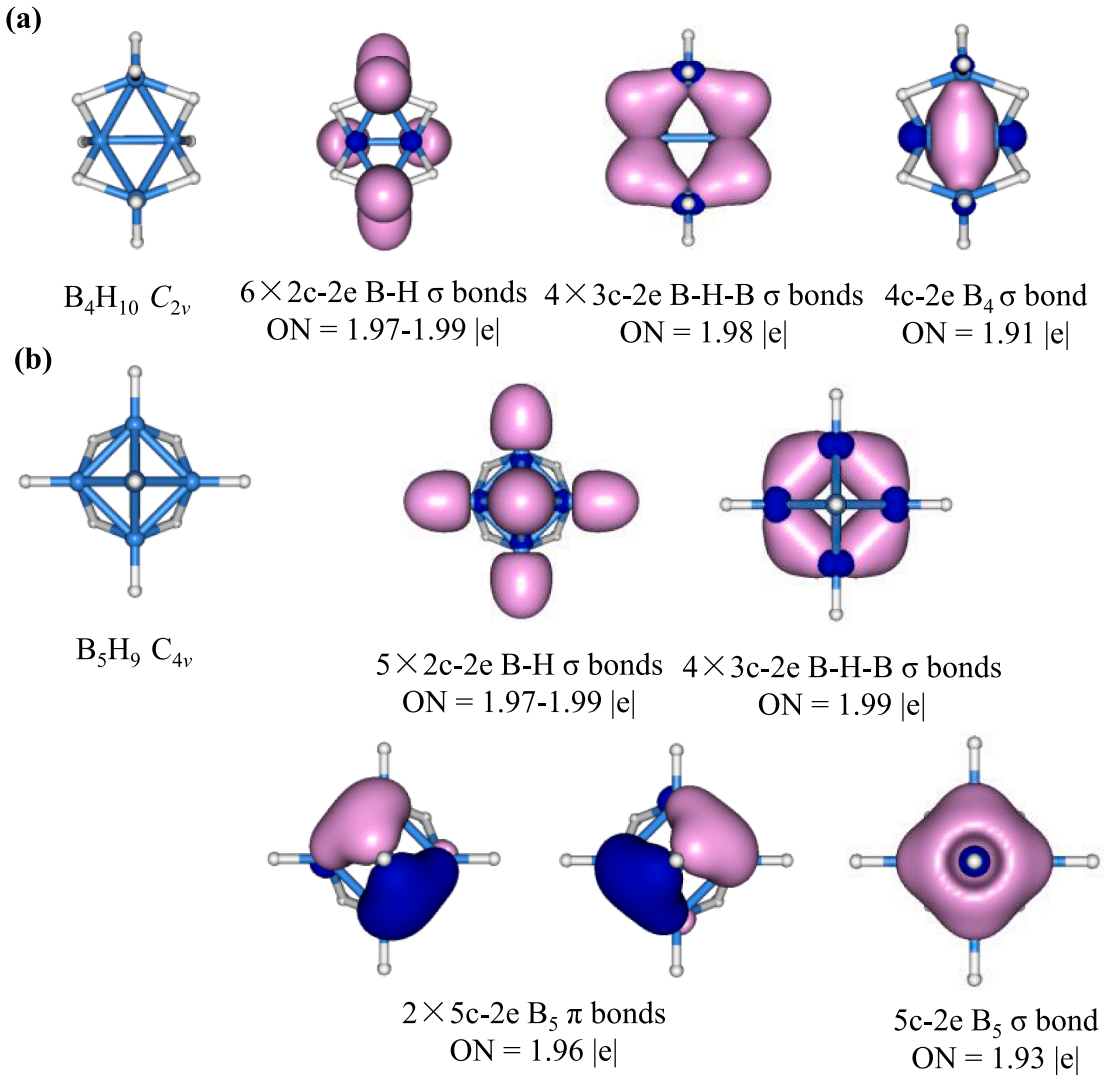

Fig. 4. Optimized structures and AdNDP chemical bonding of (a) B_4H_{10} and (b) B_5H_9 (B in blue and H in white, symmetries and occupy numbers are labeled below each structure).

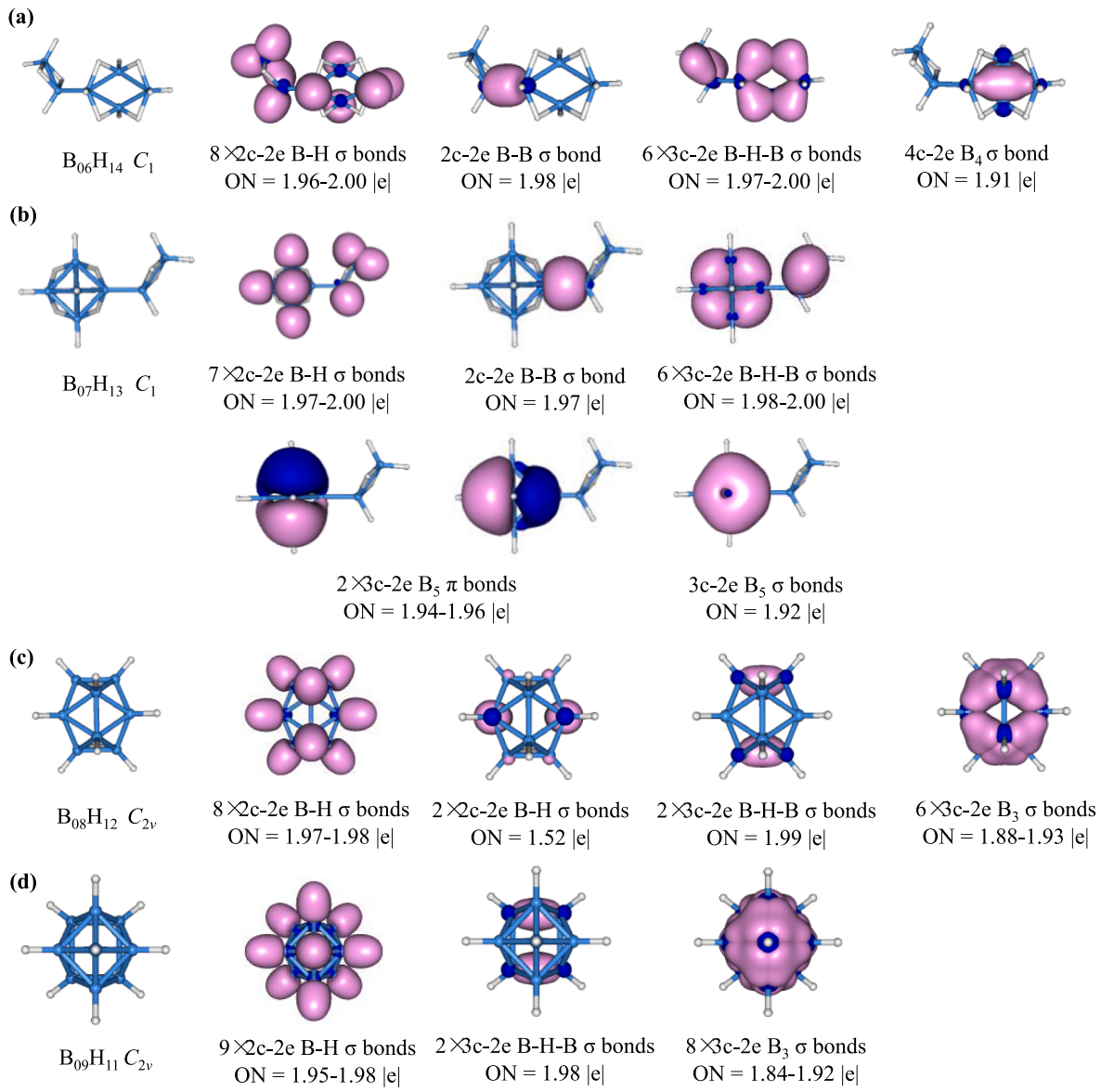

Fig. 5. Optimized structures and AdNDP chemical bonding of (a) B_6H_{14} (b) B_7H_{13} (c) B_8H_{12} and (d) B_9H_{11} (B in blue and H in white, symmetries and occupy numbers are labeled below each structure).

as the 3D open cage when $3 \leq x \leq 5$.

3.3.2. B_xH_y ($x + y = 20$, $6 \leq x \leq 9$)

With the increasing B/H ratio, more hydrogen atoms are included in the bonding systems. Therefore, there are no more separate hydrogen molecules in the B_xH_y ($x + y = 20$) clusters when $x \geq 6$. The clusters exhibit 3D open cage structure when $6 \leq x \leq 9$ (Fig. 5), and there are B—H bonds, B—H—B hydrogen-bridge bonds and multi-center σ B_n bonds in their electronic shells.

As shown in Fig. 5(a), the structure of B_6H_{14} could be viewed as the combination of D_{2h} B_2H_6 and C_{2v} B_4H_{10} through the B-B σ single bond of which the top hydrogen atom is dropped respectively, and there are eight 2c-2e σ B—H bonds, one 2c-2e σ B-B bond, six σ B—H—B hydrogen-bridge bonds and one 4c-2e σ B_4 bond in the cluster. Similarly, B_7H_{13} is combined of B_2H_6 and B_5H_9, including seven 2c-2e σ B—H bonds, one 2c-2e σ B-B bond, six σ B—H—B hydrogen-bridge bonds, and two 5c-2e π and one 5c-2e σ B_5 bonds (Fig. 5(b)). B_8H_{12} cluster includes two kinds of B—H bonds as shown in Fig. 5(c) – one kind of eight B—H bonds has the higher occupied numbers (1.97–1.98 |e|), and the other kind of the rest two B—H bonds has the relative lower occupied numbers (1.52 |e|). Moreover, it also has two B—H—B bonds and six 3c-2e σ B_3 bonds. B_9H_{11} cluster is composed of nine B—H bonds, two B—H—B bonds and eight 3c-2e σ B_3 bonds (Fig. 5(d)).

From the details of the bonding patterns in these systems, it is found that the number of *n*c-2e B_n bonds increases while the number of the hydrogen-bridgebonds decreases along with the increasing B/H ratio, which indicates the boron atoms trend to interact with each other to form the B_n multi-center bonds instead of the hydrogen-bridge bonds.

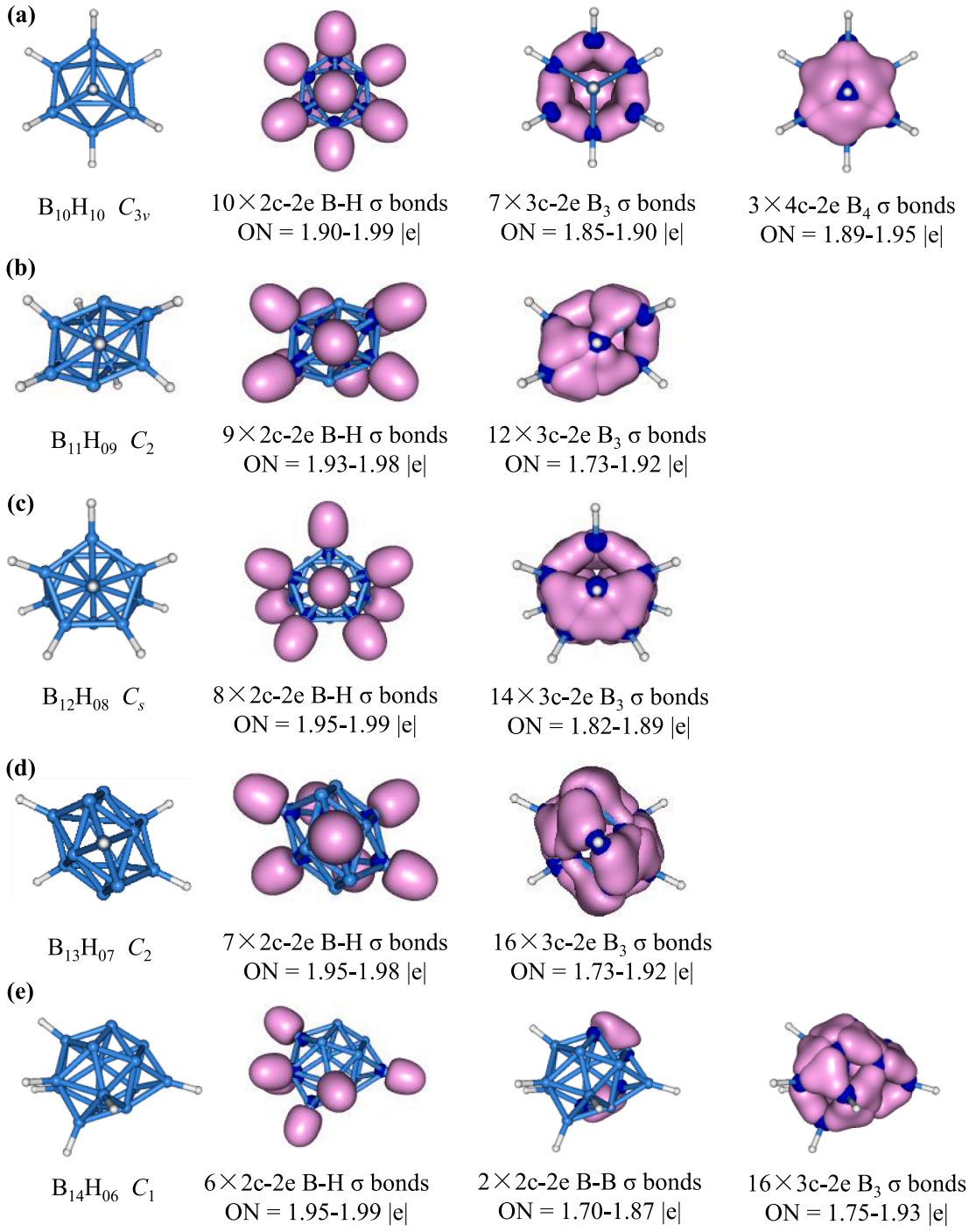

Fig. 6. Optimized structures and AdNDP chemical bonding of (a) $B_{10}H_{10}$ (b) $B_{11}H_9$ (c) $B_{12}H_8$ (d) $B_{13}H_7$ and (e) $B_{14}H_6$ (B in blue and H in white, symmetries and occupy numbers are labeled below each structure).

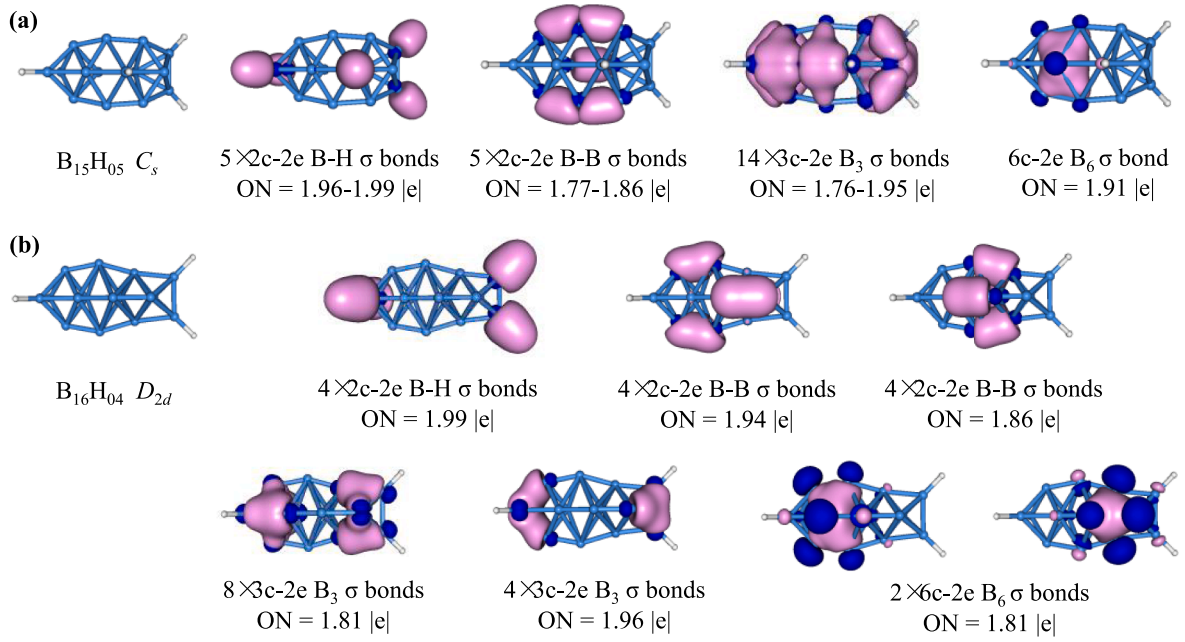

Fig. 7. Optimized structures and AdNDP chemical bonding of (a) $B_{15}H_5$ and (b) $B_{16}H_4$ (B in blue and H in white, symmetries and occupy numbers are labeled below each structure).

3.3.3. B_xH_y ($x + y = 20$, $10 \leq x \leq 16$)

When the B/H ratio reaches 1:1, the B_xH_y ($x + y = 20$) clusters are changed from the hydrogen-rich systems to the boron-rich systems. Meanwhile, their structures and bonding patterns undergo the obvious transition. On one hand, the hydrogen-bridge bonds disappear and all the hydrogen atoms are involved in the B—H single bonds. On the other hand, the boron atoms interact with each other to form the multi-center bonding systems, making their structures turn into the 3D closed cage.

In $B_{10}H_{10}$ cluster, ten hydrogen atoms are just bonded with ten boron atoms to form the B—H bonds, and the B_{10} core with unpaired electrons form the closed spherical cage structure with multi-center bonds. As shown in Fig. 6(a), the $B_{10}H_{10}$ cluster includes ten 2c-2e σ B—H single bonds, and the rest twenty valance electrons are involved in seven 3c-2e σ B_3 bonds and three 4c-2e σ B_4 bonds. $B_{11}H_9$, $B_{12}H_8$ and $B_{13}H_7$ have the similar cage structure and bonding pattern, as shown in Fig. 6(b)–(d). $B_{11}H_9$ cluster contains nine B—H bonds and twelve 3c-2e σ B_3 bonds. The B_{12} core of $B_{12}H_8$ has the stable icosahedral geometry with a slightly distortion, of which fourteen faces are occupied by 3c-2e σ B_3 bonds, the rest six are empty. Besides, there are also eight B—H bonds in the $B_{12}H_8$. $B_{13}H_7$ cluster is composed of seven B—H bonds and sixteen 3c-2e σ B_3 bonds. $B_{14}H_6$ cluster also keeps the 3D closed cage structure and its bonding pattern has a little difference (Fig. 6(e)). As the number of hydrogen atoms decreases, and the number of boron atoms with unpaired electrons further increases in the B_xH_y ($x + y = 20$) clusters, the B-B single bonds appear in the electronic shell of $B_{14}H_6$. This cluster contains six B—H bonds, two 2c-2e σ B-B bonds and sixteen 3c-2e σ B_3 bonds.

When the ratio of B/H reaches 3:1 ($x \geq 15$), $B_{15}H_5$ and $B_{16}H_4$ exhibit the 3D boat-shape closed cage structure. $B_{15}H_5$ cluster is comprised of five B—H bonds, five B-B bonds, fourteen 3c-2e σ B_3 bonds and one 6c-2e σ B_6 bond (Fig. 7(a)). $B_{16}H_4$ cluster has the similar D_{2d} configuration as B_{14} which is the magic number of neutral boron cluster, and there are four B—H bonds, eight B-B bonds, twelve 3c-2e σ B_3 bonds (two different kinds with the occupy numbers of 1.81 |e|/1.96 |e|) and two 6c-2e σ B_6 bonds (Fig. 7(b)). As the B/H ratio in B_xH_y ($x + y = 20$) further increases, the number of B-B bonds increases, while the amount of B_n multi-center bonds decreases.

3.3.4. B_xH_y ($x + y = 20$, $17 \leq x \leq 20$)

As shown in Fig. 8, the geometries of the B_xH_y ($x + y = 20$) clusters are changed into the irregular 3D when $x = 17$, 18. $B_{17}H_3$ cluster contains three 2c-2e σ B—H bonds, seven 2c-2e σ B-B bonds, fifteen 3c-2e σ B_3 bonds, one 5c-2e σ B_5 bond and one 10c-2e π bond. $B_{18}H_4$ cluster is composed of two B—H bonds, eleven B-B bonds, eleven 3c-2e σ B_3 bonds, two 5c-2e σ B_5 bonds (two different kinds with the occupy number of 1.89 |e|), one 6c-2e σ B_6 bond and one 7c-2e σ B_7 bond.

When $x = 19$, $B_{19}H$ cluster has the 2D quasi-planar structure, which could be viewed as the quasi-planar B_{18} bonded with the BH group through two 3c-2e B_3 bonds. AdNDP result in Fig. 9 reveals that there is one B—H bond, ten B-B bonds, twelve 3c-2e σ B_3 bonds, three 5c-2e σ B_5 bonds, one 6c-2e σ B_6 bond, one 18c-2e π bond and one 19c-2e π bond.

When $x = 20$, the double ring B_{20} cluster is the 2D-3D structural turning point and magic number of the neutral boron clusters. It could be viewed as the 2D folded ribbon with the special planar structure. As shown in Fig. 10, there are twenty 2c-2e σ B-B bonds, five 20c-2e delocalized σ bonds and five π bonds which include both radial and axial delocalized systems.

3.4. Transition of the geometries related with bonding patterns

As we know, neutral boron clusters B_n keep planar or quasi-planar structures until B_{20}, except for B_{14} cage as the magic number. Presence of hydrogen atoms makes planar structures less stable in B_xH_y ($x + y = 20$, $x \leq 18$). As some valence electrons in boron atoms are involved in B—H σ bonds, electronic deficiency characters are more intensive in these borane cluster, thus 3D geometries are preferred, which benefit formation of multi-center bonds. In these cage structures with various multi-center bonds, presence of empty atomic orbitals is avoided, making the clusters more stable [38]. With the increasing B/H ratio, less valence electrons are localized in B—H σ bond, and the number of multi-center B_n bonds decreases. The B-B σ bonds are formed from $B_{16}H_4$, planar geometries exist in low-lying isomers from $B_{17}H_3$, and $B_{19}H$ is the 3D-2D turning point in this series of clusters.

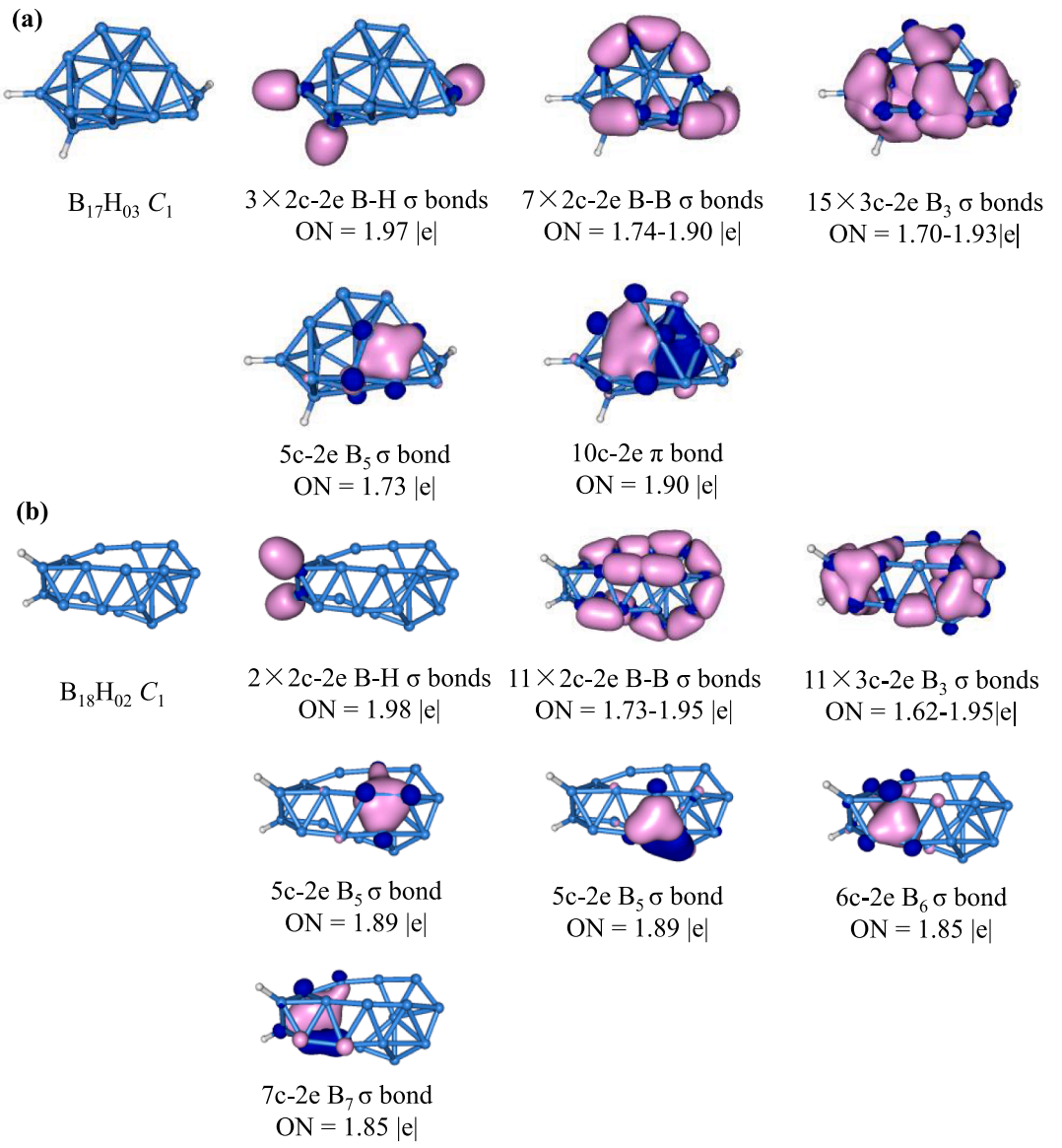

Fig. 8. Optimized structures and AdNDP chemical bonding of (a) $B_{17}H_3$ and (b) $B_{18}H_2$ (B in blue and H in white, symmetries and occupy numbers are labeled below each structure).

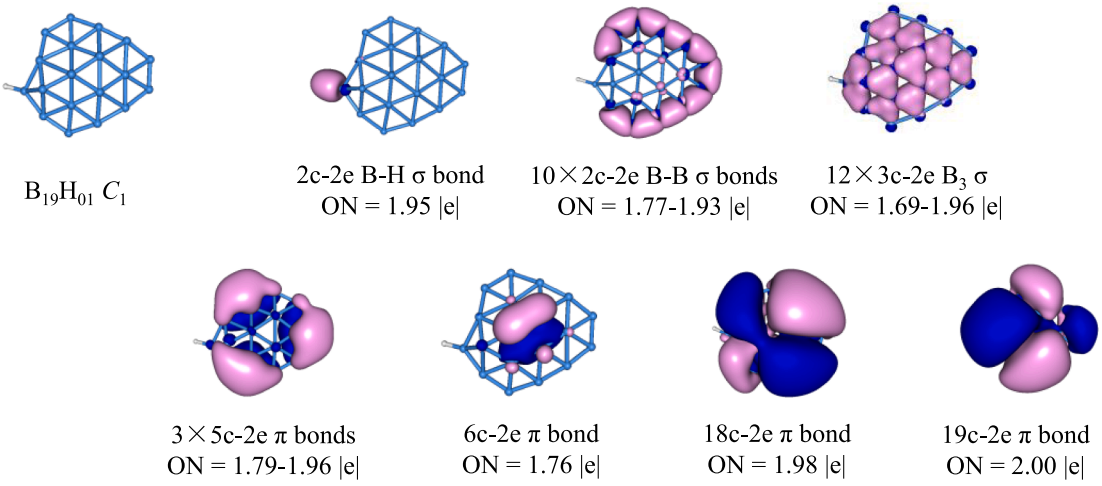

Fig. 9. Optimized structure and AdNDP chemical bonding of $B_{19}H$ (B in blue and H in white, symmetry and occupy numbers are labeled below each structure).

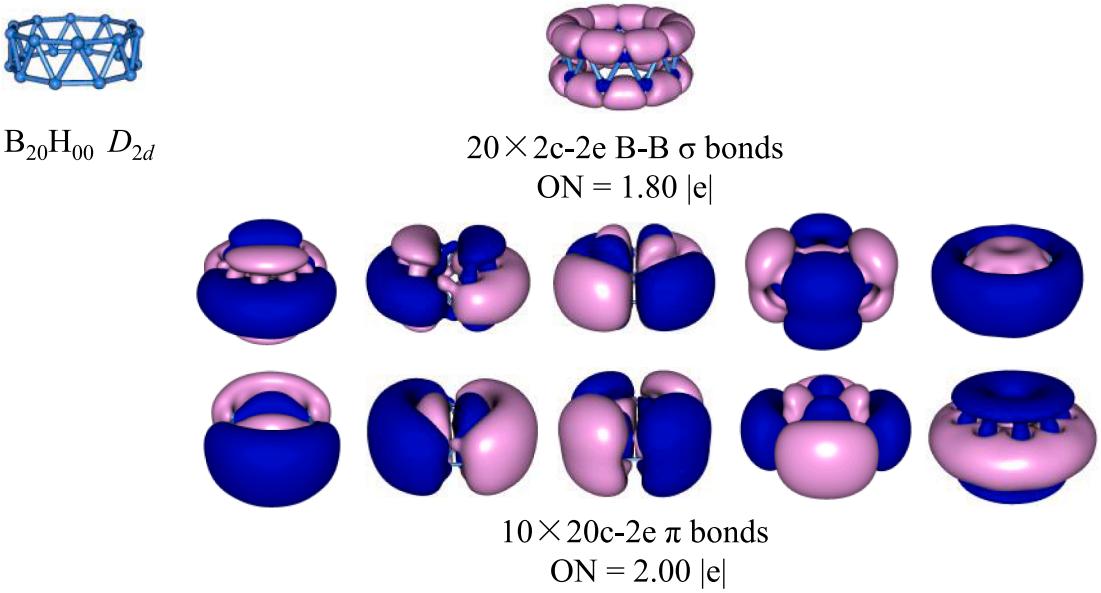

Fig. 10. Optimized structure and AdNDP chemical bonding of B_{20} (B in blue and H in white, symmetry and occupy numbers are labeled below each structure).

4. Conclusions

In this study, structural phase diagram and localized chemical bonding analysis reveal the evolution rules of geometries, energies, and bonding patterns in the B_xH_y ($x + y = 20$) systems. When $x \leq 5$, optimized systems are composed of small borane and separate hydrogen molecules. When the ratio of B/H < 1 ($x \leq 9$), the clusters have the 3D open cage structure. The hydrogen atoms are bonded with boron to form B—H single bonds and B—H—B hydrogen-bridge bonds, and the boron atoms form the multi-center B_n bonds. When the B/H ratio reaches 1:1, the hydrogen-bridge bonds disappear and the hydrogen atoms are all involved in B—H single bonds. The B_n core with diverse multi-center bonding systems forms the 3D closed cage structure. The B-B single bonds appear in the $B_{14}H_6$ and their number further increases along with the increasing B/H ratio, whereas the amount of the multi-center B_n bonds decreases. The clusters exhibit the boat-shape structure when $x =$ 15 and 16, then turn into the irregular 3D structure when $x = 17$ and 18. $B_{19}H$ is the 3D-2D turning point in these clusters with the quasi-planar structure. B_{20} with the classic double ring structure could be viewed as the folded planar ribbon. Flexible multi-center bonding patterns play an important role in the stability of these clusters, which induce the diversity of their geometries. Compared with bare boron clusters, presence of hydrogen atoms bonds some valence electrons in boron atoms, and further enhances the electronic deficiency character of the clusters. Therefore, 3D structure is more favorable before $B_{19}H$, which benefits the formation multi-center bonds. The evolution rules of geometries, energies and electronic shells in B—H binary systems gives reference for design and prediction of borane clusters, which makes sense in borane chemistry.

CRediT authorship contribution statement

Chang Xu: Investigation, Writing - original draft. **Longjiu Cheng:** Conceptualization, Software, Writing - review & editing.

Declaration of Competing Interest

The authors declare that they have no known competing financial interests or personal relationships that could have appeared to influence the work reported in this paper.

Acknowledgments

This work is financed by the National Natural Science Foundation of China (21873001), the Foundation of Distinguished Young Scientists of Anhui Province, and the Natural Science Research Project for Colleges and Universities of Anhui Province (KJ2019A0009). The calculations are carried out at the High-Performance Computing Center of Anhui University.

Appendix A. Supplementary material

Supplementary data to this article can be found online at https://doi.org/10.1016/j.comptc.2021.113194.

References

[1] W.H. Eberhardt, B. Crawford Jr, W.N. Lipscomb, The valence structure of the boron hydrides, J. Chem. Phys. 22 (1954) 989–1001.
[2] W.N. Lipscomb, The boranes and their relatives, Science 196 (1976) 1047–1055.
[3] B. Kiran, S. Bulusu, H.J. Zhai, S. Yoo, X.C. Zeng, L.S. Wang, Planar-to-tubular structural transition in boron clusters: B_{20} as the embryo of single-walled boron nanotubes, Proc. Natl. Acad. Sci. U.S.A. 102 (2005) 961–964.
[4] A.N. Alexandrova, A.I. Boldyrev, H.J. Zhai, L.S. Wang, All-boron aromatic clusters as potential new inorganic ligands and building blocks in chemistry, Coord. Chem. Rev. 250 (2006) 2811–2866.
[5] P.V.R. Schleyer, I.A. Popov, Z.A. Piazza, W.L. Li, C. Romanescu, L.S. Wang, A. I. Boldyrev, Understanding boron through size-selected clusters: Structure, chemical bonding, and fluxionality, Acc. Chem. Res. 47 (2014) 1349–1358.
[6] L.S. Wang, Photoelectron spectroscopy of size-selected boron clusters: From planar structures to borophenes and borospherenes, Int. Rev. Phys. Chem. 35 (2016) 69–142.
[7] E. Oger, N.R.M. Crawford, R. Kelting, P. Weis, M.M. Kappes, R. Ahlrichs, Boron cluster cations: Transition from planar to cylindrical structures, Angew. Chem. Int. Ed. 46 (2007) 8503–8506.
[8] L. Cheng, B_{14}: An all-boron fullerene, J. Chem. Phys. 136 (2012) 104301.
[9] Z.A. Piazza, W.L. Li, C. Romanescu, A.P. Sergeeva, L.S. Wang, A.I. Boldyrev, A photoelectron spectroscopy and *ab initio* study of B_{21}^-: Negatively charged boron clusters continue to be planar at 21, J. Chem. Phys. 136 (2012) 104310.
[10] A.P. Sergeeva, Z.A. Piazza, C. Romanescu, W.L. Li, A.I. Boldyrev, L.S. Wang, B_{22}^- and B_{23}^-: All-boron analogues of anthracene and phenanthrene, J. Am. Chem. Soc. 134 (2012) 18065–18073.
[11] I.A. Popov, Z.A. Piazza, W.L. Li, L.S. Wang, A.I. Boldyrev, A combined photoelectron spectroscopy and *ab initio* study of the quasi-planar B_{24}^- cluster, J. Chem. Phys. 139 (2013) 144307.
[12] Z.A. Piazza, I.A. Popov, W.L. Li, R. Pal, X.C. Zeng, A.I. Boldyrev, L.S. Wang, A photoelectron spectroscopy and *ab initio* study of the structures and chemical bonding of the B_{25}^- cluster, J. Chem. Phys. 141 (2014) 034303.
[13] W.L. Li, R. Pal, Z.A. Piazza, X.C. Zeng, L.S. Wang, B_{27}^-: Appearance of the smallest planar boron cluster containing a hexagonal vacancy, J. Chem. Phys. 142 (2015) 204305.

[14] Y.J. Wang, Y.F. Zhao, W.L. Li, T. Jian, Q. Chen, X.R. You, T. Ou, X.Y. Zhao, H. J. Zhai, S.D. Li, Observation and characterization of the smallest borospherene, B_{28}^- and B_{28}, J. Chem. Phys. 144 (2016) 064307.

[15] X.M. Luo, T. Jian, L.J. Cheng, W.L. Li, Q. Chen, R. Li, H.J. Zhai, S.D. Li, A. I. Boldyrev, J. Li, et al., B_{26}^-: The smallest planar boron cluster with a hexagonal vacancy and a complicated potential landscape, Chem. Phys. Lett. 683 (2017) 336–341.

[16] A.N. Alexandrova, K.A. Birch, A.I. Boldyrev, Flattening the $B_6H_6^{2-}$ octahedron. Ab initio prediction of a new family of planar all-boron aromatic molecules, J. Am. Chem. Soc. 125 (2003) 10786–10787.

[17] H.L. Yu, R.L. Sang, Y.Y. Wu, Structure and aromaticity of $B_6H_5^+$ cation: A novel borhydride system containing planar pentacoordinated boron, J. Phys. Chem. A 113 (2009) 3382–3386.

[18] Q. Chen, H. Bai, J.C. Guo, C.Q. Miao, S.D. Li, Perfectly planar concentric π-aromatic $B_{18}H_3^-$, $B_{18}H_4$, $B_{18}H_5^+$, and $B_{18}H_6^{2+}$ with [10]annulene character, Phys. Chem. Chem. Phys. 13 (2011) 20620–20626.

[19] N.G. Szwacki, C.J. Tymczak, $B_{12}H_n$ and $B_{12}F_n$: Planar vs icosahedral structures, Nanoscale Res. Lett. 7 (2012) 1–6.

[20] D.Z. Li, Q. Chen, Y.B. Wu, H.G. Lu, S.D. Li, Double-chain planar D2h B4H2, C2h B8H2, and C2h B12H2: conjugated aromatic borenes, Phys. Chem. Chem. Phys. 14 (2012) 14769–14774.

[21] H. Bai, Q. Chen, C.Q. Miao, Y.W. Mu, Y.B. Wu, H.G. Lu, H.J. Zhai, S.D. Li, Ribbon aromaticity in double-chain planar $B_nH_2^{2-}$ and $Li_2B_nH_2$ nanoribbon clusters up to n = 22: Lithiated boron dihydride analogues of polyenes, Phys. Chem. Chem. Phys. 15 (2013) 18872–18880.

[22] W.L. Li, C. Romanescu, T. Jian, L.S. Wang, Elongation of planar boron clusters by hydrogenation: Boron analogues of polyenes, J. Am. Chem. Soc. 134 (2012) 13228–13231.

[23] H. Bai, Q. Chen, Y.F. Zhao, Y.B. Wu, H.G. Lu, J. Li, S.D. Li, $B_{30}H_8$, $B_{39}H_6^{2-}$, $B_{42}H_{10}$, $B_{48}H_{10}$, and $B_{72}H_{12}$: Polycyclic aromatic snub hydroboron clusters analogous to polycyclic aromatic hydrocarbons, J. Mol. Model. 19 (2013) 1195–1204.

[24] E.D. Jemmis, E.G. Jayasree, Analogies between boron and carbon, Acc. Chem. Res. 36 (2003) 816–824.

[25] Q. Chen, S.D. Li, π-aromatic $B_{16}H_6$: A neutral boron hydride analogue of naphthalene, J. Cluster Sci. 22 (2011) 513–523.

[26] D.Z. Li, H.G. Lu, S.D. Li, Planar π-aromatic C3h B6H3+ and π-antiaromatic C2h B8H2: Boron hydride analogues of D3h C3H3+ and D2h C4H4, J. Mol. Model. 18 (2012) 3161–3167.

[27] W.J. Tian, H. Bai, H.G. Lu, Y.B. Wu, S.D. Li, Planar D2h B26H8, D2h B26H82+, and C2h B26H6: Building blocks of stable boron sheets with twin-hexagonal holes, J. Cluster Sci. 24 (2013) 1127–1137.

[28] A.N. Alexandrova, E. Koyle, A.I. Boldyrev, Theoretical study of hydrogenation of the doubly aromatic B_7^- cluster, J. Mol. Model. 12 (2006) 569–576.

[29] M. Böyükata, C. Özdoğan, Z.B. Güvenç, Effects of hydrogen hosting on cage structures of boron clusters: Density functional study of B_mH_n (m = 5–10 and n ≤ m) complexes, Phys. Scr. 77 (2008) 025602.

[30] T.B. Lee, M.L. McKee, Redox energetics of *hypercloso* boron hydrides B_nH_n (n = 6–13) and $B_{12}X_{12}$ (X = F, Cl, OH, and CH_3), Inorg. Chem. 51 (2012) 4205–4214.

[31] F. Klanberg, D.R. Eaton, L.J. Guggenberger, E.L. Muetterties, Chemistry of boranes. XXVIII. New polyhedral borane anions, $B_8H_8^{2-}$, $B_8H_8^{\cdot-}$, and $B_7H_7^{2-}$, Inorg. Chem. 6 (1967) 1271–1281.

[32] S. Kalvoda, B. Paulus, M. Dolg, H. Stoll, H.J. Werner, Electron correlation effects on structural and cohesive properties of *closo*-hydroborate dianions $(B_nH_n)^{2-}$ (n = 5–12) and B_4H_4, Phys. Chem. Chem. Phys. 3 (2001) 514–522.

[33] J.A. Wunderlich, W.N. Lipscomb, Structure of $B_{12}H_{12}^{2-}$ ion, J. Am. Chem. Soc. 82 (1960) 4427–4428.

[34] M. Joshi, T.K. Ghanty, Lanthanide and actinide doped $B_{12}H_{12}^{2-}$ and $Al_{12}H_{12}^{2-}$ clusters: New magnetic superatoms with f-block elements, Phys. Chem. Chem. Phys. 21 (2019) 23720–23732.

[35] Y.F. Shen, C. Xu, L.J. Cheng, Deciphering chemical bonding in $B_nH_n^{2-}$ (n = 2–17): Flexible multicenter bonding, RSC Adv. 7 (2017) 36755–36764.

[36] Y. Ohishi, K. Kimura, M. Yamaguchi, N. Uchida, T. Kanayama, Energy barrier of structure transition from icosahedral $B_{12}H_6^+$ to planar $B_{12}H_5^+$ and $B_{12}H_4^+$ clusters, J. Phys.: Conf. Ser. 176 (2009) 012030.

[37] H. Bai, S.D. Li, Hydrogenation of $B_{12}^{0/-}$: A planar-to-icosahedral structural transition in $B_{12}H_n^{0/-}$(n =1–6) boron hydride clusters, J. Cluster Sci. 22 (2011) 525–535.

[38] J.K. Olson, A.I. Boldyrev, Planar to 3D transition in the B_6H_y anions, J. Phys. Chem. A 117 (2013) 1614–1620.

[39] W.N. Lipscomb, Boron Hydrides, W. A. Benjamin, New York, 1963.

[40] D.S. Marynick, W.N. Lipscomb, Fractional 3-center bonds in carboranes, J. Am. Chem. Soc. 94 (1972) 1748–1750.

[41] D.A. Dixon, D.A. Kleier, T.A. Halgren, W.N. Lipscomb, Localized molecular-orbitals for polyatomic-molecules.4. Large boron hydrides, J. Am. Chem. Soc. 98 (1976) 2086–2096.

[42] D.A. Dixon, D.A. Kleier, T.A. Halgren, W.N. Lipscomb, Localized orbitals in large boron hydrides – $B_{16}H_{20}$ and related molecules, J. Am. Chem. Soc. 96 (1974) 2293–2295.

[43] D.A. Dixon, D.A. Kleier, T.A. Halgren, J.H. Hall, W.N. Lipscomb, Localized orbitals for polyatomic-molecules. 5. Closo boron hydrides $B_nH_n^{2-}$ and carboranes $C_2B_{n-2}H_n$, J. Am. Chem. Soc. 99 (1977) 6226–6237.

[44] J.H. Hall, D.A. Dixon, D.A. Kleier, T.A. Halgren, L.D. Brown, W.N. Lipscomb, Localized molecular-orbitals for polyatomic-molecules. 2. Structural relationships and charge-distributions for open boron hydrides and ions, J. Am. Chem. Soc. 97 (1975) 4202–4213.

[45] D.Y. Zubarev, A.I. Boldyrev, Developing paradigms of chemical bonding: Adaptive natural density partitioning, Phys. Chem. Chem. Phys. 10 (2008) 5207–5217.

[46] E. Osorio, J.K. Olson, W. Tiznado, A.I. Boldyrev, Analysis of why boron avoids sp^2 hybridization and classical structures in the B_nH_{n+2} series, Chem.-Eur. J. 18 (2012) 9677–9681.

[47] K. Wade, The structural significance of the number of skeletal bonding electron-pairs in carboranes, the higher boranes and borane anions, and various transition-metal carbonyl cluster compounds, J. Chem. Soc. D: Chem. Commun. 15 (1971) 792–793.

[48] E.D. Jemmis, M.M. Balakrishnarajan, P.D. Pancharatna, A unifying electron-counting rule for macropolyhedral boranes, metallaboranes, and metallocenes, J. Am. Chem. Soc. 123 (2001) 4313.

[49] R. Liao, R. Sa, Y. Zhu, Q. Li, A topological pattern for understanding the structures of boranes and borane analog compounds, Struct. Chem. 26 (2015) 353–364.

[50] M.A. Beckett, B. Brellochs, I.T. Chizhevsky, T. Damhus, K.H. Hellwich, J.D. Kennedy, R. Laitinen, W.H. Powell, D. Rabinovich, C. Vinas; et al., Nomenclature for boranes and related species (IUPAC Recommendations 2019), Pure Appl. Chem. 92 (2020) 355–381.

[51] J. Aihara, Three-dimensional aromaticity of polyhedral boranes, J. Am. Chem. Soc. 100 (1978) 3339–3342.

[52] P.V.R. Schleyer, K. Najafian, A.M. Mebel, The large closo-borane dianions, BnHn2-(n = 13-17) are aromatic, why are they unknown? Inorg. Chem., 37 (1998) 6765–6772.

[53] J. Aihara, Aromatic character of deltahedral borane dianions revisited, Inorg. Chem. 40 (2001) 5042–5044.

[54] R.B. King, Three-dimensional aromaticity in polyhedral boranes and related molecules, Chem. Rev. 101 (2001) 1119–1152.

[55] N.G. Szwacki, V. Weber, C.J. Tymczak, Aromatic borozene, Nanoscale Res. Lett. 4 (2009) 1085–1089.

[56] J. Poater, M. Solà, C. Viñas, F. Teixidor, Hückel's rule of aromaticity categorizes aromatic *closo* boron hydride clusters, Chem.-Eur. J. 22 (2016) 7437–7443.

[57] W. Lu, D.C.H. Do, R. Kinjo, A flat carborane with multiple aromaticity beyond Wade-Mingos' rules, Nat. Commun. 11 (2020).

[58] B. Bai, H. Bai, Structural transition upon hydrogenation of B_{20} at different charge states: From tubular to disk-like, and to cage-like, Phys. Chem. Chem. Phys. 18 (2016) 6013–6020.

[59] W. An, S. Bulusu, Y. Gao, X.C. Zeng, Relative stability of planar versus double-ring tubular isomers of neutral and anionic boron cluster B_{20} and B_{20}^-, J. Chem. Phys. 124 (2006) 154310.

[60] J.M. Tao, J.P. Perdew, V.N. Staroverov, G.E. Scuseria, Climbing the density functional ladder: Nonempirical meta-generalized gradient approximation designed for molecules and solids, Phys. Rev. Lett. 91 (2003).

[61] Y. Yuan, L.J. Cheng, Theoretical prediction for the structures of gas phase lithium oxide clusters: $(Li_2O)_n$ (n=18), Int. J. Quantum Chem. 113 (2013) 1264–1271.

[62] L. Li, L. Cheng, First principle structural determination of $(B_2O_3)_n$ (n = 1–6) clusters: From planar to cage, J. Chem. Phys. 138 (2013) 094312.

[63] W.J. Wei, P.E.M. Siegbahn, The active E4 structure of nitrogenase studied with different DFT functionals, J. Comput. Chem. 42 (2021) 81–85.

[64] T.B. Tai, M.T. Nguyen, The B_{32} cluster has the most stable bowl structure with a remarkable heptagonal hole, Chem. Commun. 51 (2015) 7677–7680.

[65] D.Y. Zubarev, A.I. Boldyrev, Revealing intuitively assessable chemical bonding patterns in organic aromatic molecules via adaptive natural density partitioning, J. Org. Chem. 73 (2008) 9251–9258.

[66] T.R. Galeev, B.D. Dunnington, J.R. Schmidt, A.I. Boldyrev, Solid state adaptive natural density partitioning: A tool for deciphering multi-center bonding in periodic systems, Phys. Chem. Chem. Phys. 15 (2013) 5022–5029.

[67] M.J. Frisch, G.W. Trucks, H.B. Schlegel, G.E. Scuseria, M.A. Robb, J.R. Cheeseman, G. Scalmani, V. Barone, B. Mennucci, G.A. Petersson; et al., GAUSSIAN 09, Revision B.01, Gaussian, Inc., Wallingford, CT, Gaussian Inc., Wallingford, CT, 2009.

[68] U. Varetto, Molekel 5.4.0.8, Swiss National Supercomputing Centre, Manno, Switzerland, 2009.

[69] A.B. Burg, H.I. Schlesinger, Hydrides of boron. VII. Evidence of the transitory existence of borine (BH_3): Borine carbonyl and borme trimethylammine, J. Am. Chem. Soc. 59 (1937) 780–787.

[70] T.P. Fehlner, W.S. Koski, The dissociation of BH_3CO into BH_3 and CO, J. Am. Chem. Soc. 87 (1965) 409–413.

[71] N.N. Greenwood, R. Greatrex, Kinetics and mechanism of the thermolysis and photolysis of binary boranes, Pure Appl. Chem. 59 (1987) 857–868.